Designation: F2603 – 06 (Reapproved 2012)

Standard Guide for Interpreting Images of Polymeric Tissue Scaffolds[1]

This standard is issued under the fixed designation F2603; the number immediately following the designation indicates the year of original adoption or, in the case of revision, the year of last revision. A number in parentheses indicates the year of last reapproval. A superscript epsilon (ε) indicates an editorial change since the last revision or reapproval.

1. Scope

1.1 This guide covers the factors that need to be considered in obtaining and interpreting images of tissue scaffolds including technique selection, instrument resolution and image quality, quantification and sample preparation.

1.2 The information in this guide is intended to be applicable to porous polymer-based tissue scaffolds, including naturally derived materials such as collagen. However, some materials (both synthetic and natural) may require unique or varied sample preparation methods that are not specifically covered in this guide.

1.3 The values stated in SI units are to be regarded as standard. No other units of measurement are included in this standard.

1.4 *This standard does not purport to address all of the safety concerns, if any, associated with its use. It is the responsibility of the user of this standard to establish appropriate safety and health practices and to determine the applicability of regulatory limitations prior to use.*

2. Referenced Documents

2.1 *ASTM Standards:*[2]

E1919 Guide for Worldwide Published Standards Relating to Particle and Spray Characterization (Withdrawn 2014)[3]

E2245 Test Method for Residual Strain Measurements of Thin, Reflecting Films Using an Optical Interferometer

F1854 Test Method for Stereological Evaluation of Porous Coatings on Medical Implants

F1877 Practice for Characterization of Particles

F2150 Guide for Characterization and Testing of Biomaterial Scaffolds Used in Tissue-Engineered Medical Products

F2450 Guide for Assessing Microstructure of Polymeric Scaffolds for Use in Tissue-Engineered Medical Products

3. Terminology

3.1 *Definitions:*

3.1.1 *aliasing, n*—artifactual data that originates from an insufficient sampling rate.

3.1.2 *biomaterial, n*—a natural or synthetic material that is suitable for introduction into living tissue especially as part of a medical device, such as an artificial heart valve or joint.

3.1.3 *blind (end) pore, n*—a pore that is in contact with an exposed internal wall or surface through a single orifice smaller than the pore's depth.

3.1.4 *closed cell, n*—void within a solid, lacking any connectivity with an external surface. Synonym: *closed pore*.

3.1.5 *feret diameter, n*—the mean value of the distance between pairs of parallel tangents to the periphery of a pore (adapted from Practice F1877).

3.1.6 *hydrogel, n*—a water-based open network of polymer chains that are cross-linked either chemically or through crystalline junctions or by specific ionic interactions.

3.1.7 *irregular, adj*—an irregular pore that cannot be described as round or spherical. A set of reference figures that define the nomenclature are given in Appendix X2. (Adapted from Practice F1877).

3.1.8 *Nyquist criterion*—a criterion that states that a signal must be sampled at a rate greater than or equal to twice its highest frequency component to avoid aliasing.

3.1.9 *permeability, n*—a measure of fluid, particle, or gas flow through an open pore structure.

3.1.10 *pixel, n*—two-dimensional picture element.

3.1.11 *polymer, n*—a long chain molecule composed of monomers.

3.1.11.1 *Discussion*—A polymer may be a natural or synthetic material.

3.1.11.2 *Discussion*—Examples of polymers include collagen and polycaprolactone.

3.1.12 *pore, n*—a liquid, fluid, or gas-filled externally connecting channel, void, or open space within an otherwise solid or gelatinous material (for example, textile meshes composed

[1] This guide is under the jurisdiction of ASTM Committee F04 on Medical and Surgical Materials and Devicesand is the direct responsibility of Subcommittee F04.42 on Biomaterials and Biomolecules for TEMPs.

Current edition approved Oct. 1, 2012. Published February 2007. DOI: 10.1520/F2603-06.

[2] For referenced ASTM standards, visit the ASTM website, www.astm.org, or contact ASTM Customer Service at service@astm.org. For *Annual Book of ASTM Standards* volume information, refer to the standard's Document Summary page on the ASTM website.

[3] The last approved version of this historical standard is referenced on www.astm.org.

of many or single fibers (textile-based scaffolds), open cell foams, (hydrogels). Synonyms: *open pore, through pore*.

3.1.13 *porosity, n*—property of a solid which contains an inherent or induced network of channels and open spaces. Porosity can be determined by measuring the ratio of pore (void) volume to the apparent (total) volume of a porous material and is commonly expressed as a percentage (Guide F2150).

3.1.14 *rectangular, adj*—A pore that approximates a square or rectangle in shape (derived from Practice F1877).

3.1.15 *roundness (R), n*—a measure of how closely an object represents a circle (Practice F1877).

3.1.16 *scaffold, n*—a support, delivery vehicle, or matrix for facilitating the migration, binding, or transport of cells or bioactive molecules used to replace, repair, or regenerate tissues. (Guide F2150).

3.1.17 *segmentation, n*—a methodology for distinguishing different regions (for example, pores and walls) within a tissue scaffold image.

3.1.18 *spherical pore, n*—a pore with a generally spherical shape.

3.1.18.1 *Discussion*—A spherical pore appears round in a photograph (Practice F1877).

3.1.19 *threshold, n*—isolation of a range of grayscale values exhibited by one constituent within an image.

3.1.20 *through pores, n*—an inherent or induced network of voids or channels that permit flow of fluid from one side of the structure to the other.

3.1.21 *tortuosity, n*—a measure of the mean free path length of through pores relative to the sample thickness. Alternative definition: The squared ratio of the mean free path to the minimum possible path length.

3.1.22 *voxel, n*—three-dimensional picture element.

4. Significance and Use

4.1 This document provides guidance for users who wish to obtain quantifiable data from images of tissue scaffolds manufactured from polymers that include both high water content gels and woven textiles.

4.2 Information derived from tissue scaffold images can be used to optimize the structural characteristics of the matrix for a particular application, to develop better manufacturing procedures or to provide a measure of quality assurance and product traceability. Fig. 1 provides a summary of the key stages of image capture and analysis.

4.3 There is a synergy between the analysis of pores in tissue scaffolds and that of particles that is reflected in standards cited and in the analysis described in Section 9. Guide E1919 provides a compendium of standards for particle analysis that includes measurement techniques, data analytical and sampling methodologies.

5. Measurement Objectives

5.1 Much of the research activity in tissue engineering is focused on the development of suitable materials and structures for optimal growth of a range of tissue types including cartilage, bone, and nerve. This requires a quantitative assessment of the scaffold structure.

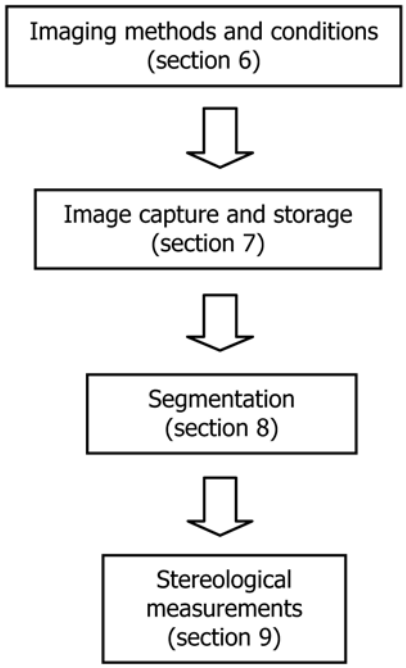

FIG. 1 Key Stages in Image Capture, Storage, and Analysis

The key parameters that need to be determined are (*1*) the overall level of porosity, (*2*) the pore size distribution, which can range from tens of nanometers to several hundred micrometres, and (*3*) the degree of interconnectivity and tortuosity of the pores.

6. Imaging Methods and Conditions

6.1 There are many experimental ways of obtaining key scaffold physical parameters as described in Guide F2450. When imaging and subsequent quantitative analysis is chosen as the method for determining these parameters, it is critical that any image under consideration be a true representation of the scaffold of interest. Some imaging methods require sample preparation. Some do not. When sample preparation is required prior to imaging, care must be taken that the procedures do not significantly alter the morphology of the scaffold. See Appendix X1 for further information on sample preparation.

6.2 Images obtained using techniques such as light microscopy, electron microscopy, and magnetic resonance imaging are two-dimensional (2-D) representations of a three-dimensional (3-D) structure. These can be a planar or cross-sectional view with a relatively large depth of field or a series of physical or virtual 2-D slices, each with a small depth of field, that can be reassembled in a virtual environment to produce a 3-D mesostructure.

6.3 There are limits to the extent an image (2-D or 3-D) can faithfully represent the physical artifacts that are influenced by factors germane to the imaging method, such as spatial resolution and dynamic range, image contrast, and the signal-to-noise ratio. Table 1 lists some of the techniques available for

TABLE 1 Sources of Contrast and Techniques to Generate Images of Tissue Scaffolds

Generic method	Contrast source	Maximum resolution (lateral/axial)	Physical slicing required for 3D imaging?
Widefield Optical Microscopy	Refractive index Fluorescence Absorbance	1 μm/(10 μm)	Y
Confocal Optical Microscopy	Refractive index Fluorescence Absorbance	0.5 μm/1 μm	N
Optical Coherence Tomography (or Microscopy)	Refractive index	1 μm/1 μm	N
Scanning Acoustic Microscopy (SAM)	Acoustic impedance	0.1 μm/0.1 μm (depending on the wavelength chosen)	N
Magnetic Resonance Imaging (MRI)	Nuclear spin	10 μm/10 μm	N
X-ray Micro-Computed Tomography (μ-CT)	Electron density	10 μm/10 μm	N
Transmission Electron Microscopy (TEM)	Electron density	Approximately 0.2 nm in plane	Y
Scanning Electron Microscopy (SEM)	Electron density	Approximately 10 nm	N

producing images of porous structures, along with their contrast source, maximum demonstrated spatial resolution, and typical dynamic range. Proper technique selection depends both on the material properties of the scaffold (that is, optical methods cannot be used with opaque materials) the contrast available, and the target pore size range.

6.4 The images generated by the techniques shown in Table 1 cannot reproduce features smaller than the spatial resolution of the method. Features that are faint, that is, those that do not have significant contrast, or signal significantly above background, will be resolved at length scales larger than the maximum resolution. Excessive contrast can also limit the penetration depth due to scattering effects. This is particularly true of optical microscopies using differences in refractive index as the contrast mechanism. An appropriate level of contrast that can be established by experimentation is therefore critical to high quality imaging.

6.5 Contrast can be enhanced by using exogenous agents, such as florescence tags in optical microscopy and stains containing heavy metal complexes in electron microscopies. Excessive contrast can be ameliorated in optical microscopies by imbibing the structure with a fluid that has an index of refraction similar to that of the solid making up the structure (this is termed "index-matching"). There are many excellent resources describing factors influencing widefield and confocal optical microscopy (**1-3**),[4] optical coherence microscopy (**4**), MRI (**5**), and electron microscopies (**6**).

6.6 The reconstruction of the mesostructure in 3-D from a series of 2-D images obtained from a sample that has been physically sectioned requires considerably more effort than assembly of virtual sections produced by techniques that are able to focus on a plane within the sample. The virtual approach is also less prone to sample distortion since it obviates the need for physical sectioning and registration errors in the reassembly process. However, the techniques used to generate virtual 2-D images typically have limited penetration depth.

6.7 Confocal microscopy (OCT), for example, has a penetration depth of approximately 100 μm, a value that depends on the wavelength of the light used and the amount of scattering that occurs within the sample. Scanning acoustic microscopy (SAM) can extend the penetration depth to approximately 1 mm in polymer scaffolds albeit with a reduction in image resolution.

6.8 In general, using longer wavelength radiation to improve penetration of the radiation is accompanied by a reduction in resolution.

7. Image Capture and Storage

7.1 Image acquisition in this guide refers to the process of capturing an image through digitization that is then stored for subsequent analysis. Care should be taken during this stage to avoid loss of fidelity by controllable factors that are not related to the methodology used to produce the image. These factors include the spatial sampling frequency of the detector system, the dynamic range of analogue to digital (A/D) conversion, segmenting (thresholding) operations (discussed in Section 9), and both image compression and decompression.

7.2 Spatial sampling frequency and appropriate A/D conversion are straightforward issues; the sampling frequency should be at least twice the inverse spatial resolution, so as to fulfill the Nyquist criterion. Sampling at frequencies below this will lead to the display of artifacts. Most image processing systems have anti-aliasing filters that remove frequencies greater than $F_s/2$ Hz, where F_s is the digital sampling rate. The A/D conversion should utilize a sufficient number of bits to cover the dynamic range of the imaging / detector system. Eight-bit conversion and recording is used for most common imaging applications, resulting in images with 256 grayscale levels, where 0 corresponds to pure black and 255 to pure white respectively. If 8-bit conversion is used in a color (RGB) image there are 256 possible color combinations.

NOTE 1—The gamut, or range of the grayscale reflects the image contrast.

7.3 It is important to record the minimum measurement value (that is, the dimensions of a single pixel) when using digital capture or digitizing film-based images at all magnifications used in measurements (Test Method F1854).

7.4 Image compression is used to facilitate rapid display of data and easy file transmission. However, many compression methods (JPEG, PNG, and GIF) cause a loss of data. This loss generally occurs in the high-frequency components of the spatial Fourier spectrum of the image, leading to an oscillating, smeared grayscale, or color intensity profile at the object edges. Some proprietary compression methods are purported to involve no loss of information and thus be completely reversible

[4] The boldface numbers in parentheses refer to a list of references at the end of this standard.

(7). There are excellent internet resources describing compression and decompression techniques (7).

7.5 After capture, an image can be manipulated to facilitate subsequent analysis. Such transformations include noise suppression, enhancement of regions that are of particular interest, and corrections that compensate for instrument or experimental limitations.

7.6 *Noise Suppression*—The minor random fluctuations in signal intensity or noise that are present in digitized images can degrade the quality of the image if the contrast between the material and background is low. Averaging a number of frames, *N*, can significantly reduce noise levels. The invariant signal intensity increases with respect to *N* whilst the intensity of the random noise only increases by the square root of *N*. The signal-to-noise ratio, *Sn*, therefore scales as $N/\sqrt{N}$.

7.7 *Background Correction*—Lack of homogeneity of the illuminating source can occur across a sample due to the source itself or a nonlinear response of the detector. This can be compensated for by subtracting a background captured in the absence of a sample from the image.

7.8 *Spatial-domain Filtering* refers to enhancement of desired features in an image accomplished through working in the spatial domain. For example, in mask mode radiography, an X-ray image is obtained of an area before and after a contrast agent is added. The former image is subtracted from the latter, and the result is an image with the feature of interest amplified over the background. Other examples of spatial domain filtering include opening and closing, which simply add or subtract a pixel width to the periphery of a defined area. By cycling opening and closing operations, features can be enhanced or noise near an interface can be eliminated.

7.9 *Frequency-domain Filtering:*

7.9.1 In frequency-domain filtering, filtering operations are performed on the 2-D or 3-D Fourier or similar transformation of an image plane. The data is subsequently transformed back into real space to give the filtered image.

7.9.2 Care should be taken to store the original data file before modifying the image through any kind of manipulation or filtering.

8. Segmentation

8.1 Tissue scaffold images are often in or converted to monochrome that spans a grayscale ranging from near black to near white (for example Fig. 2). The solid and void components of the scaffold will be represented by values at opposite ends of the grayscale (Fig. 3). Intermediate shades of gray represent the transition in brightness that occurs as the solid component terminates into pores. An initial step in any morphological analysis of such an image is to establish a criterion for segmenting those regions of the image that correspond to the solid, or 'wall' and the void, or 'pore' respectively.

8.2 There are many methods for segmenting image areas belonging to pore and solid (8). The most straightforward approach is to define a grayscale threshold, in which the solid appears as nearly white. Grayscale values below the threshold

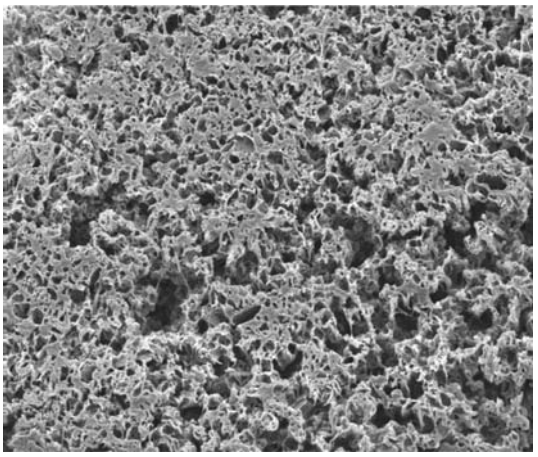

FIG. 2 Low-Contrast Micrograph of Polycaprolactone PCL Scaffold

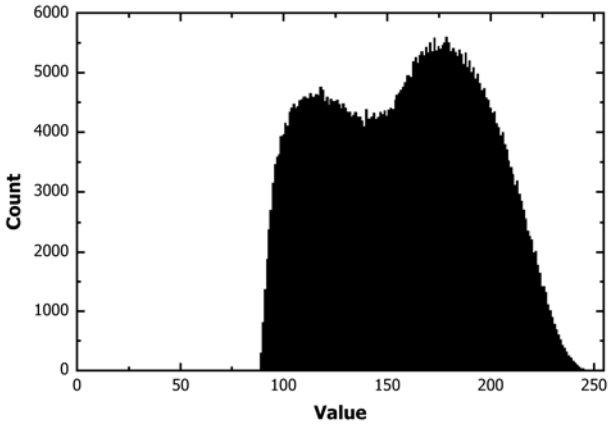

NOTE 1—Corresponding to image shown in Fig. 2.

FIG. 3 Bimodal Histogram of Grayscale Intensities

are assigned to represent pores, and all others to represent the walls of the structure.

8.3 The threshold grayscale intensity can also be determined manually, a task that can be made easier by increasing the image contrast if it does not cover the full gamut from 0 to 255. This manipulation of the image data is straightforward and can be found in image analysis software packages. An inevitable consequence of this action, if performed on a stored image, is to introduce periodic gaps into the grayscale histogram.

8.4 Methods have also been developed for objective threshold assignment based on statistical analysis of histograms (9). Many of these approaches assume a normal distribution for pixels associated with the pores and a second normal distribution for pixels associated with the walls which may or may not be an acceptable assumption. Otsu (10) has proposed a method that does not rely on these probabilistic density distributions. The approach utilizes the variance as a measure of homogeneity. The threshold is determined by minimizing the variance in the pixels associated with the pores and walls respectively.

8.5 Other segmentation methods that are based on the detection of edges, or regions, are available. These approaches utilize texture or brightness as indicators of change and are

especially useful in interpreting images where contrast between the subject and the background is poor. One such method is the marching cubes algorithm (**11**).

9. Stereological Measurements

9.1 Once the grayscale image has been segmented and reduced to a binary (black and white) image it can be analyzed in terms of the shape and size and the size distribution of the black domains, which correspond to the pores. Stereological measurements provide quantitative data on, for example, the volume fraction of pores, the number of pores per unit area, as well as size information and the degree of interconnectivity. The interconnectvity is a measure of how well the pores are connected to each other; high values for interconnectivity do not necessarily equate to high permeability. The path length between adjacent pores can be tortuous (see 9.10).

9.2 *Pore Shape (Morphology):*

9.2.1 There are several quantities which are specifically defined to characterize pore morphology. These include equivalent circle diameter (ECD), aspect ratio (AR), elongation (E), roundness (R), and form factor (FF). Each of these quantities focuses on a particular aspect of pore morphology, depending on its mathematical definition. Appendix X2 demonstrates several pore shapes and the corresponding values of each of these, and the mathematical definitions of each are shown below.

9.2.2 *The aspect ratio* is the ratio of the major diameter, d_{max}, that is, the longest line that can be drawn between two points on an outline to the minor diameter, d_{min}. The minor diameter is defined as the longest line perpendicular to the major diameter that connects two points on the outline.

9.2.3 *The elongation* is similar to the aspect ratio and is defined as the ratio of the pore length to the average pore width. It is particularly useful for characterizing long pores where the major axis line does not stay within the pore boundaries.

9.2.4 *The roundness, R*, provides a measure of the circularity of a pore. A perfect circle has a roundness of 1. *R* is calculated from the area of the pore (A), and the maximum diameter (d_{max}) according to

$$R = (4A)/(\pi d_{max}^2) \quad (1)$$

9.2.5 *The form factor, FF*, is also a measure of pore circularity that uses the perimeter of the pore outline, p, rather than d_{max}, that is

$$FF = 4\pi A/p^3 \quad (2)$$

9.3 *Pore Size and Aspect Ratio Based on Feret Diameters*—The particle size and aspect ratio is given by the mean of two Feret diameters. This approach is particularly useful when quantifying round and rectangular pores.

9.4 *Pore Size Based on Equivalent Circle Diameters*—The area of an irregularly shaped pore, *A*, can be expressed in terms of an ECD. The correspondence between the ECD and the actual diameter of a pore obviously improves with increasing roundness of pores. The ECD is given by

$$ECD = (4 \cdot A/\pi)^{1/2} \quad (3)$$

9.5 *Analysis of Irregularly Shaped Pores:*

9.5.1 Pore size and shape analysis discussed in paragraphs 9.2 through 9.4 implicitly assume an almost spherical pore shape. While such pore geometries are common, there are many examples where this is not the case. Nonspherical pores may be random shapes or severely elongated. A common approach to analyzing such pore morphologies is to (digitally) find the spheres of maximal diameter that still fit entirely within the pore at a particular point; this procedure is carried out along the pore. The locus of sphere centers gives the skeletonized center of the pore and the distribution of sphere radii gives a measure of the pore diameter.

9.5.2 Pores of regular, nonspherical shape are best characterized by comparison with an ideal pore shape. This approach was taken in characterization of porosity/permeability reference scaffolds that are being developed through ASTM Task Group F04.42.06 (**12**). In brief, an ideal pore geometry is defined, and unit cells are extracted from an image based on this geometry. The size of the unit cell or deviations from ideal shape can then be characterized. Figures displaying a cubic porous scaffold and related unit cells are given in Appendix X3.

9.6 *Assessment of Porosity:*

9.6.1 Measures of the porosity can be obtained in both 2-D and 3-D. The 2-D calculation is made by dividing the area occupied by pores by the total area of the image; this can be simply done by determining the ratio of pixels associated with the pores, PP_i to the number contained in the whole image, PP_t (see Test Method E2245). The volume fraction, V_p, is equal to the area fraction as defined by

$$V_p = A_p = A_p/A_t = PP_i/PP_t \quad (4)$$

where:

A_p = total area of all the pores in the image, and
A_t = the image area.

9.6.2 The *volume fraction* can also be expressed as a percentage by multiplying the area or point fraction by 100 (see Test Method E2245).

9.6.3 The 3-D equivalent is a measure of the void volume in a given volume of sample. In both cases there will be uncertainty in the measured values due to ambiguities in defining edges as well as other experimental considerations (Section 10).

9.7 Software packages that automatically carry out area analyses require the user to define a lower limit for the number of pixels that constitute a pore. This provides a crude noise filter and will contribute to the uncertainty of subsequent calculations.

9.8 Determination of the pore sizes and level of porosity will be affected by factors that include the homogeneity of the size and shape of the pores and their orientation with respect to the image, as shown in Fig. 4. Such issues are less important for random pore sizes and shapes.

9.9 The magnification of the captured image should be constant when comparing different samples within a series. Guidance on the most suitable magnification for capturing images is given in Table 2. Once the image has been captured, it can then be viewed at any magnification.

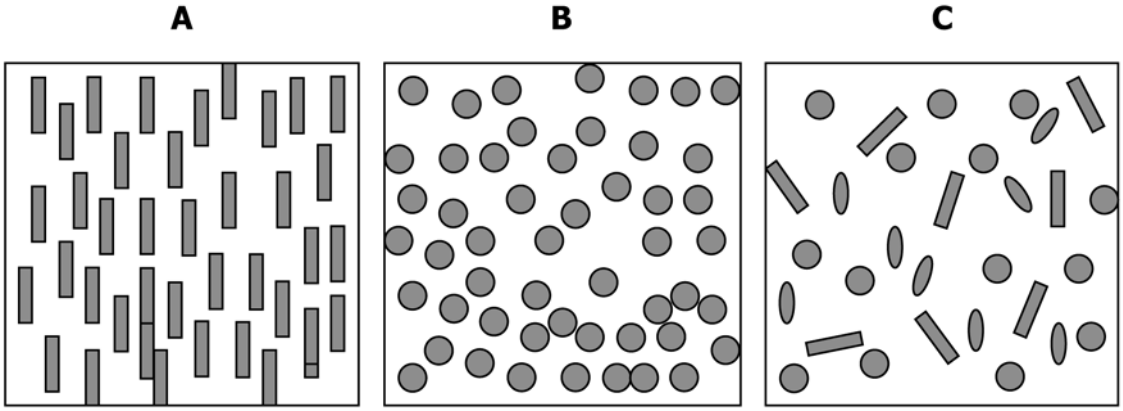

NOTE 1—The pore morphology, size and porosity of oriented samples can be very sensitive to the image orientation as shown above in A and B for rod-like pores. This is less important for irregular or randomly oriented structures, C.

FIG. 4 Pore Morphology, Size and Porosity of Oriented Samples

TABLE 2 Recommended Magnifications for Imaging Pores

NOTE 1—This information is based on particle analysis methods described in Practice F1877.

Magnification	Pore size range (μm)
10 000	0.1 to 1.0
1000	1 to 10
100	10 to 100

9.10 *Assessment of Interconnectivity and Tortuosity:*

9.10.1 The ability of nutrients to reach living cells residing on a tissue scaffold depends on several factors, including pore size and pore volume fraction; these parameters are discussed above. Two other relevant parameters are tortuosity and pore interconnectivity. The former describes the path that a tracer particle would take as it passes from one point to another through the scaffold of interest, or equivalently, the curvedness of a skeletonized pore structure. (See Note 2.) There are many ways to define tortuosity. Two examples are (*1*) sum of angles, where the angles are defined by three points along a skeletonized pore backbone; these angles are along a backbone and are normalized by the path length; and (*2*) inflection count, where inflection points along a skeletonized pore backbone are counted and this number (plus one) is multiplied by the total path length of the pore or path and then divided by the distance between endpoints.

NOTE 2—A skeletonized pore structure shows the spatial location of pores.

9.10.2 Interconnectivity of an elongated pore is also an important morphological parameter, and can be defined simply by the number of pore crossings per unit length along a skeletonized pore backbone.

9.11 *Classification of Pores*—Pores can be classified as open (through), closed (enclosed), or blind-ended, depending on whether or not they connect with an external surface as shown in Fig. 5. All of these pores are important in determining the performance of the scaffold. Open pores provide conduits for cell migration and are key to successful nutrient/waste product flow. Closed pores and blind-end pores can make a significant contribution to meeting cellular requirements for oxygen and dispersal of carbon dioxide. All three pores are important in influencing the degradation behavior of the scaffold.

FIG. 5 Schematic Representation of Different Pore Types that Can Exist within a Tissue Scaffold

10. Precision and Bias

10.1 All measurements are subject to random errors that are beyond the control of the experimenter or systematic which directly reflects the way in which the experiment is conducted. Analysis of segmented images to quantify the number of pores, the pore area or volume, or if 3-D sections are available, is prone to systematic error due to bias in selecting interesting regions of the image to study or exclusion of pores that exceed a certain size. In gathering image data care should be taken to ensure that sufficient randomly selected images are gathered to provide statistically meaningful data that represents the sample.

10.2 The number of specimens required to achieve this objective depends on the method used and an interaction between the magnification used and the distribution of pore sizes. The area contained within an electron micrograph can range from 1 μm^2 or less to several square millimeters. Further guidance on this topic can be found in reference (**9**).

10.3 The analysis of 3-D virtual images that are recreated from a series of serial 2-D images brings additional choice, that is, choosing the distance between successive slices that will be a compromise between resolution and time spent both in acquiring data and analyzing it.

10.4 Reliable procedures for validating data derived from the analysis of tissue scaffold images have yet to be identified. Repeatedly analyzing the same image using different settings for, for example, the threshold intensity and criterion for excluding pixels, can be used to produce a qualitative assessment of the robustness of the procedures used in the analysis. Comparison of the variance within these data will provide an indication of the sensitivity of the analysis to different parameters.

10.5 Comparisons of data obtained from different regions of the sample can be used as a measure of structural homogeneity.

10.6 Calibration of equipment and procedures is required if the data produced are to be traceable. Equipment should be calibrated whenever appropriate and reference materials (that is, particles or scaffold materials) should be utilized if available.

11. Keywords

11.1 biomaterials; image analysis; matrix, scaffold; polymeric; segmentation; stereological analysis; thresholding; tissue scaffolds

APPENDIXES

(Nonmandatory Information)

X1. SAMPLE PREPARATION AND ARTIFACTS

X1.1 There are many potential ways to distort the morphology of an artifact during sample preparation, for example:

X1.1.1 Sudden changes in pressure can damage delicate structures containing gas pockets. These can occur if the samples are subjected to vacuum during the process of imbibing index-matching fluid for optical imaging. As a precaution, these should be evacuated very slowly.

X1.1.2 The morphology of delicate structures that contain a significant amount of water can easily be distorted if freezing from aqueous solution is part of the preparation process. This distortion can be due to water expansion and/or a dramatic change in the balance of thermodynamic forces that drive self-assembly (such as are important to the structure of hydrogels). When it is critical to protect the scaffold structure from rupture due to expansion of ice, hydrophilic glassformers such as small-molecule and polymeric sugars or poly-alcohols can be incorporated into the scaffold to prevent freezing. Rapid cooling (for example, a slush nitrogen quench) can be used to freeze in the structure of thermodynamically sensitive materials such as hydrogels.

X1.1.3 Microtoming, if not properly performed, can stress and distort morphology.

X1.1.4 Care should be taken to avoid using fluids for refractive index matching or embedding that can distort the polymer matrix as a result of absorption or water loss.

X2. PORE MORPHOLOGY—QUANTIFICATION

X2.1 Fig. X2.1 shows a comparison of equivalent circle diameters for different pore morphologies together with other quantifiable measures of shape.

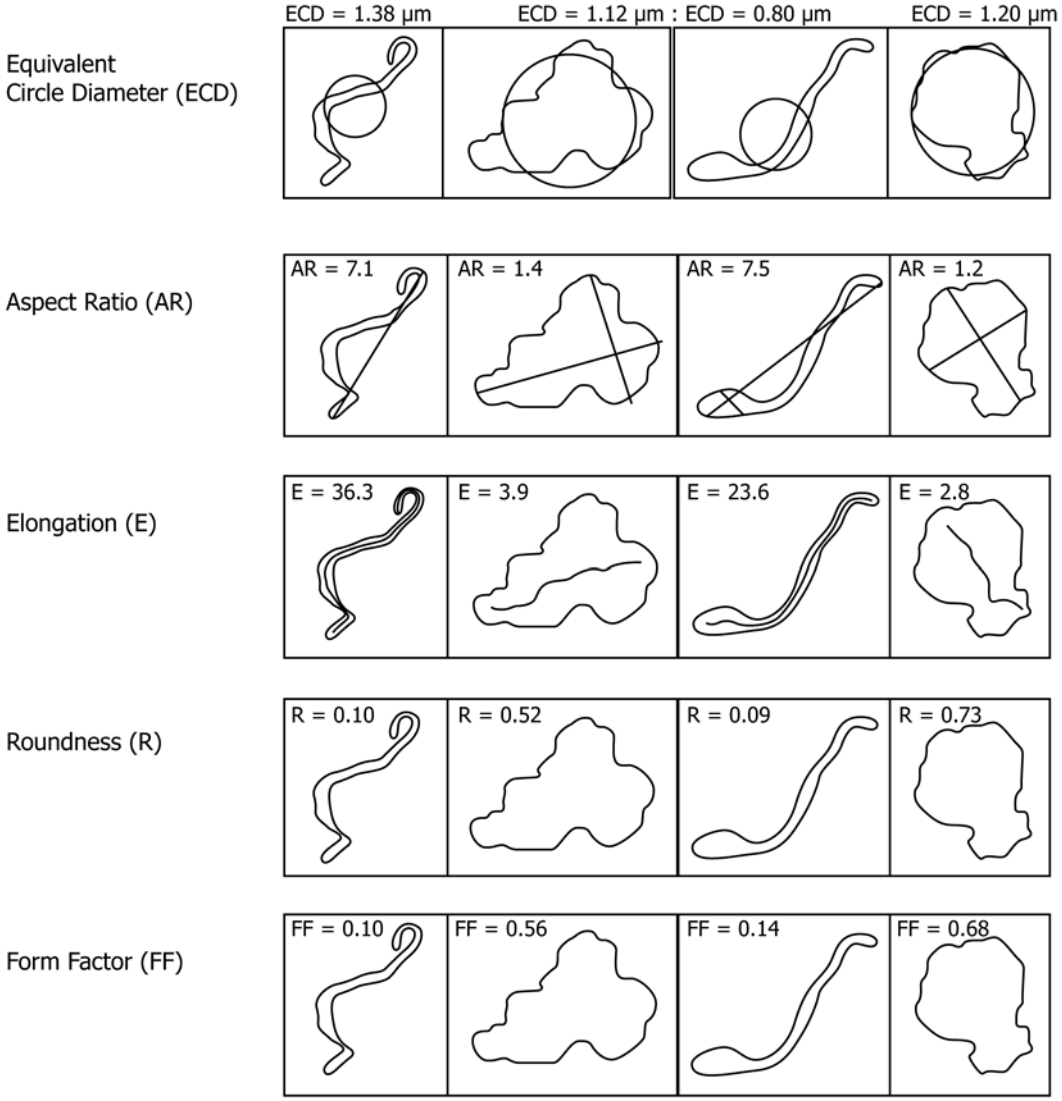

FIG. X2.1 Relationship between Different Pore Shapes and Characterization Parameters (From Practice F1877)

X3. QUANTIFICATION OF NONSPHERICAL PORES

X3.1 Fig. X3.1 is an image of a cubic porous structure. Fig. X3.2 (a) through (d) are pore shapes that are found within such a structure. Cells such as depicted in Fig. X3.2 (a) are found within the body of the cubic structure; those typical of Fig. X3.2 (b) are found in cells touching only one external wall. Cells in Fig. X3.2 (c) are found at edges (touching two external walls), and cells of the type shown in Fig. X3.2 (d) are found at vertices.

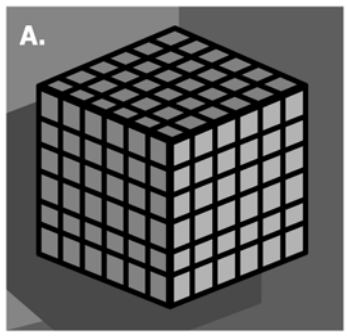

FIG. X3.1 Cubic Porous Structure

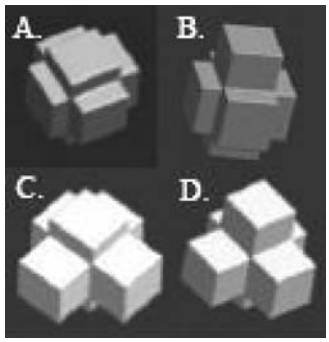

FIG. X3.2 Shapes of Unit Cells Found within the Cubic Porous Structure shown in Fig. X3.1

REFERENCES

(1) http://www.microscopyu.com/ (The Nikon company optical microscopy website has educational tutorials on, for example, confocal microscopy.)

(2) http://www.olympusmicro.com/primer/ (An introduction to microscopy can be found at the Olympus company website.)

(3) Wilson, T. and Sheppard, C. J. R., *Theory and Practice of Scanning Optical Microscopy* , Academic Press, New York, 1984.

(4) Bouma, B. E. and Tearney, G. J., eds, *Handbook of Optical Coherence Tomography*, Marcel Dekker, Inc, New York, 2002.

(5) Brown , M. and Semelka, R. C., *MRI: Basic Principles and Applications*, 2nd Edition, Wiley- Liss, 1995.

(6) Slayter, E. M. and Slayter, H. S., *Light and Electron Microscopy*, Cambridge University Press, 1992.

(7) http://datacompression.info/ImageCompression.shtml. (An example of a site that is a resource provider of text books, programs, discussion groups and other informative sites concerned with data compression.)

(8) Clarke, A. R. and Eberhardt, C. N., *Microscopy Techniques for Materials Science*, Woodhead Publishing, Cambridge, UK and CRC Press, Florida, USA, 2002.

(9) Russ, J. C., *Computer Assisted Microscopy in the Measurement and Analysis of Images*, Plenum Press, 1992.

(10) Otsu, N. "A threshold selection method from gray level," *IEEE Trans. Systems, Man and Cybernetics*, 1979, Vol 9, p. 62.

(11) Lorensen, W. and Cline, H. E., "Marching Cubes: A High Resolution 3D Surface Construction Algorithm," *Computer Graphics (SIGGRAPH 87 Proceedings)*, Vol 21(4), July 1987, pp. 163–170.

(12) ASTM Task Group F04.42.06, ASTM WK6507: Development of Reference Scaffolds for Tissue Engineering.